

# QUANTUM DOTS-SENSITIZED SOLAR CELL: SILAR CYCLES EFFECT ON THE PARAMETERS OF PHOTOVOLTAIC

T. T. Ha<sup>1\*</sup>, Q. V. Lam<sup>1</sup>, T. D. Huynh<sup>1</sup>

<sup>1</sup>University of Science, Vietnam National University - HCM City, Vietnam

**Abstract:** The photovoltaic performance of quantum dot-sensitized solar cells (QDSSCs) based on mesoscopic TiO<sub>2</sub> spheres. A series of CdS/CdSe/ZnS co-sensitized TiO<sub>2</sub> photoanodes for QDSSCs were prepared by successive ionic layer adsorption and reaction (SILAR) processes. The growth of CdS, CdSe and ZnS layers were monitored by taking UV-Visible absorption spectra and the SILAR cycles of CdS, CdSe and ZnS show different impact on the performance of QDSSCs. With the deposition times of CdS, CdSe changing (from 1 to 5 cycles), the parameters of the device is changed. In addition to determine the quality of QDSSCs, we used modern physical methods to calculate the dynamic resistance values as  $R_s$ ,  $R_{sh}$ ,  $R_b$ ,  $R_D$ . The effect of SILAR cycles on the dynamic resistance was discussed detail.

**Keywords** - Photovoltaic, SILAR.

## 1. INTRODUCTION

The third generation photovoltaic based on QDs resolve the Shockley-Queisser limit and low cost photovoltaic. It develops based on many p-n junctions and applicates the QDs to replace dyes. The results obtained the performance of 40% [1]. In recent years, scientists have discovered the QDs which can create the high performance solar cells [2]. The QDs can be changed the particle size, leading to the change in the absorption spectrum [3]. Controlling the size of QDs, we can change their absorption spectrum. Furthermore, QDs have the ability to associate with biological molecules to transfer charge faster while reducing losses and helping passivated surface (reduced defect states) of them. In 1990, Vogel and colleagues have applicated CdS QDs with Pt cathode to collect the low efficiency [4]. Although not high performance, but this is a new direction in research QDSSCs. Then, a series of studies aimed at process improvement such as replacement of different quantum dots, TiO<sub>2</sub> semiconductor materials, electrolyte, counter electrodes to enhance the performance photovoltaic [5,6,7]. Lee and colleagues have studied on CdSe, CdTe QDs using Pt counter electrode as result as the efficiency of under 1% in 2007 [8]. One year later, a series of studies by Lee and colleagues on systems CdS, CdSe QDs improved the performance by up to 1.2% when using polysulfide electrolyte [7]. During this time, the group of Lopez-Luke, Mora-Sero, Shen, Tachibana synthesized CdS, CdSe QDs with Pt counter electrode but different electrolyte systems (Na<sub>2</sub>S, NaOH + Na<sub>2</sub>S + S) to get the highest performance of 2.2%. In 2009, 2010, 2011, 2012, a various QDSSCs were studied by the scientists. Cheng has prepared on CdS and CdSe co sensitized TiO<sub>2</sub> nanowires and nanorods using Na<sub>2</sub>S+Na<sub>2</sub>SO<sub>3</sub> electrolyte. A high efficiency was obtained of up to 2.41% in 2012 [9]. Although there was much research as listed. However, there are no the studies about the mechanisms processes (combination processes, electron transport processes in the semiconductor film and at junctions, the process of corrosion of the electrode anode by electrolyte) and the influence of resistances on the performance QDSSCs.

In this paper, we prepared CdS/CdSe/ZnS co-sensitizer on mesoporous TiO<sub>2</sub> surfaces with different SILAR cycles. The optical

properties of the photoanodes and the photovoltaic performance of the corresponding solar cells were investigated. In addition to determine the quality of QDSSCs, we used modern physical methods to calculate the dynamic resistance values as  $R_s$ ,  $R_{sh}$ ,  $R_b$ ,  $R_D$ . The effect of SILAR cycles on the dynamic resistance was discussed detail.

## 2. EXPERIMENT

### 2.1 Materials

Cd(CH<sub>3</sub>COO)<sub>2</sub>·2H<sub>2</sub>O (99%), KCl, Na<sub>2</sub>S, Zn(NO<sub>3</sub>)<sub>2</sub>, Se powder, S powder, Na<sub>2</sub>SO<sub>3</sub>, TiCl<sub>4</sub>, TiO<sub>2</sub> paste obtained from Dyesol, Australia. FTO (Fluorine-doped tin oxide) obtained from Nippon Sheet Glass company (8 Ω/square).

### 2.2 Preparation on sensitized TiO<sub>2</sub> films

The TiO<sub>2</sub> films were coated by layers TiO<sub>2</sub> by silk-screen printing. The TiO<sub>2</sub> films were annealed at 500°C for 30 min. Their sizes ranged from 10 to 30 nm (TEM image in Fig 1a). The thickness of TiO<sub>2</sub> films was around 4 μm measured by Stylus spectra. Then, the TiO<sub>2</sub> film was dipped in 40-mmol TiCl<sub>4</sub> solution for 30 min at 70°C and sintered at 500°C for 30 min. The specific surface area of the mesoporous TiO<sub>2</sub> was investigated by using the N<sub>2</sub> adsorption and desorption isotherms before and after the calculation. The surface area is 120.6 m<sup>2</sup>g<sup>-1</sup> (measured by BET devices). This result indicates that the synthesized material has wider mesoporous structure.

### 2.3 Preparation TiO<sub>2</sub>/CdS/CdSe/ZnS films

The TiO<sub>2</sub>/CdS/CdSe/ZnS films were synthesized by SILAR method as follow: Firstly, the TiO<sub>2</sub> film was dipped in 0.5 M Cd<sup>2+</sup>-ethanol solution for 1 min and rinsed with ethanol. Then, it was dipped for 1 min in 0.5 M S<sup>2-</sup>-methanol solution and rinsed with methanol after drying in the air (a cycle SILAR). Amount of CdS QDs was increased by repeating the assembly cycles from one to five cycles. The secondly, the TiO<sub>2</sub>/CdS was dipped into 1M Cd<sup>2+</sup>-ethanol solution for 1 min at room temperature and rinsed with ethanol. Then, it was dipped for 1 min in 0.5 M Se<sup>2-</sup>-aqueous solution and rinsed with pure water after drying in the air (a cycle SILAR). Amount of CdSe QDs was increased by repeating the assembly cycles from one to five cycles. For the ZnS passivation layer, the TiO<sub>2</sub>/CdS/CdSe films were dipped into 0.1 M Zn<sup>2+</sup>-

## Publication History

Manuscript Received : 25 June 2014  
Manuscript Accepted : 28 June 2014  
Revision Received : 29 June 2014  
Manuscript Published : 30 June 2014

solution and 0.1 M S<sup>2-</sup>-solutions for 1 min and rinsed with pure water between two dips (a total of two cycles). Finally, it was annealed in a vacuum environment with different temperatures to avoid oxidation. The TiO<sub>2</sub>/CdS/CdSe/ZnS was being measured thickness by the Stylus spectra. The results of the average thickness of the CdS (3 cycles), CdSe (3 cycles), ZnS (2 cycles) are 351.9 nm, 56.1 nm, 257.8 nm respectively. The coating of F<sup>-</sup> ions was performed by dipping the TiO<sub>2</sub> photoelectrode into a 1 M NH<sub>4</sub>F aqueous solution for 2 min, rinsed by de-ionized water. Two layers of F<sup>-</sup> ions were coated: the first was coated before the deposition of CdS QDs, the second after the deposition of three layers of QDs and the same for CdSe. The images and structure of the QDSSCs show in Fig 1.

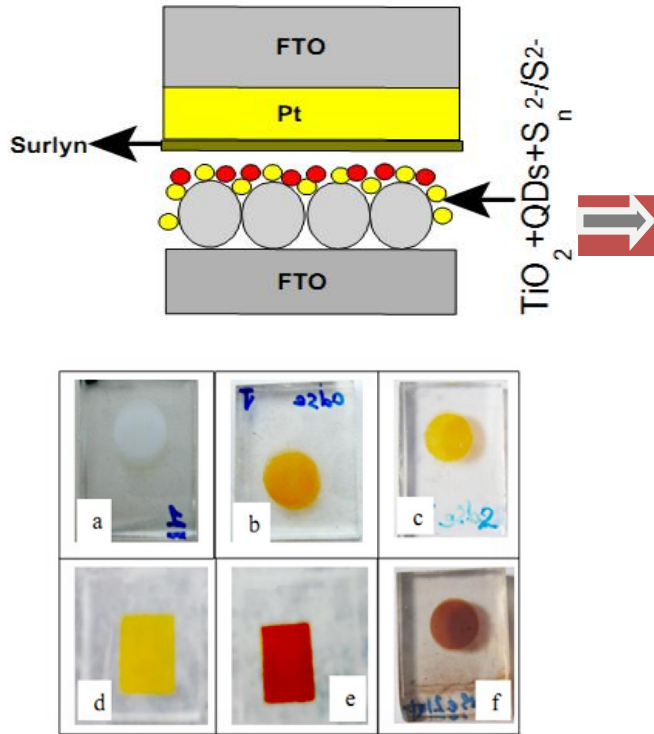


Fig 1. The diagram shows the instruction of the QDSSCs

### 2.4 Fabrication of QDSSCs

The structure of QDSSCs was designed by the photoanodes and counter electrodes using a Surlyn at 170°C. The electrolyte was filled from a hole made on the counter electrode. The active area of QDSSCs was 0.38 cm<sup>2</sup>. The polysulfide electrolyte was 0.5 M Na<sub>2</sub>S, 0.2 M S and 0.2 M KCl in Milli-Q ultrapure water/methanol (7:3 by volume).

### 2.5. Characterizations and measurements

The morphology of the prepared samples was observed using TEM device. The crystal structure was analyzed with an X-ray diffractometer (Philips, Panalytical X'pert, CuKα radiation). The absorption properties of the nanotube array samples were investigated using a diffuse reflectance UV-vis spectrometer (JASCO V-670). Photocurrent – Voltage measurements were performed on a Keithley 2400 sourcemeter using a simulated AM 1.5 sunlight with an output power of 100 mW/cm<sup>2</sup> produced by a solar simulator (Solarena, Sweden).

### 2.6. The determination of dynamic resistance photovoltaic

A dynamic of the QDSSCs can be schematically represented as in Fig 2. This is a new method to determine dynamic resistance from illuminated one I-V curve. We used this method to calculate the

dynamic resistance values as R<sub>S</sub>, R<sub>SH</sub>, R<sub>d</sub>, R<sub>D</sub>. Then, the effect of SILAR cycles on the dynamic resistance.

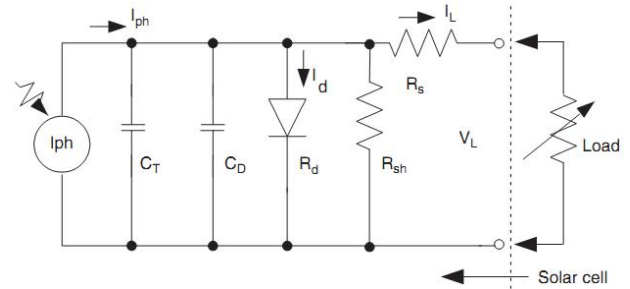


Fig 2. AC equivalent circuit of a solar cell

We determine the resistance of the photovoltaic from the measurement I-V curve by the equations following [10]:

> Under one illumination level

$$R_S = \frac{V_1 - V_2}{I_2 - I_1} - \frac{1}{\alpha(I_2 - I_1)} \ln \left[ \frac{I_{ph} + I_0 - I_1}{I_{ph} + I_0 - I_2} \right] = R_D - R_d \quad (1)$$

$$R_D = \frac{V_1 - V_2}{I_2 - I_1} \quad (2)$$

$$R_d = \frac{1}{\alpha(I_2 - I_1)} \ln \left[ \frac{I_{ph} + I_0 - I_1}{I_{ph} + I_0 - I_2} \right] \quad (3)$$

$$R_{SH} = \frac{V_{OC}}{I_{ph} - I_0(e^{qV_{OC}/kT} - 1)} \quad (4)$$

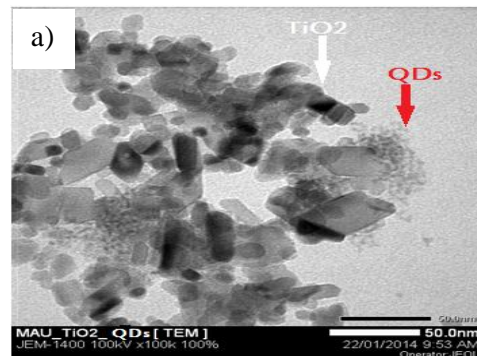
> Under dark conditions

$$R_S = -\frac{V_1 - V_2}{I_2 - I_1} + \frac{1}{\alpha(I_2 - I_1)} \ln \left[ \frac{I_0 - I_1}{I_0 - I_2} \right] = R_d - R_D \quad (5)$$

With R<sub>S</sub>, R<sub>SH</sub>, R<sub>d</sub>, R<sub>D</sub> are series resistance, shunt resistance, internal dynamic and external dynamic correspond. I<sub>ph</sub>, I<sub>0</sub> are the diode reverse saturation current and the photocurrent, α=q/nKT. The operating points (V<sub>1</sub>, I<sub>1</sub>), (V<sub>2</sub>, I<sub>2</sub>) on a single I-V curve.

## 3. RESULTS AND DISCUSSION

Detailed morphological features and crystallinity of the pure TiO<sub>2</sub> and TiO<sub>2</sub>/CdS/CdSe/ZnS photoanodes were investigated using a TEM image. Fig. 3a shows a TEM image of the TiO<sub>2</sub>/CdS/CdSe/ZnS photoanode prepared with the SILAR cycle number of CdS, CdSe and ZnS at 3 layers, 3 layers and 2 layers. We can clearly see that QDs uniformly cover the surface of TiO<sub>2</sub> nanoparticles. It shows that the mean diameter of QDs is from 2 nm to 3 nm. The results of the TEM demonstrate that the SILAR method is an efficient TiO<sub>2</sub> sensible strategy for obtaining well covering the QDs on the TiO<sub>2</sub> surface.



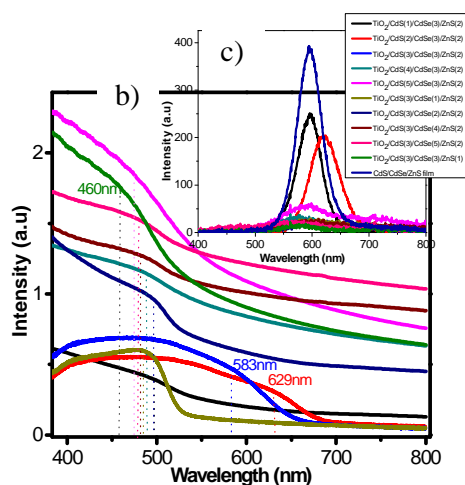


**Fig 3.** (a) Image TEM, (b) UV-Vis absorption spectra of the  $\text{TiO}_2/\text{CdS}/\text{CdSe}/\text{ZnS}$  photoanodes sensitized by CdS/CdSe/ZnS QDs show the light absorption behavior of photoanodes changed with the SILAR cycles of CdS, CdSe and ZnS and (c) Photoluminescence (PL) spectra of the  $\text{TiO}_2/\text{CdS}/\text{CdSe}/\text{ZnS}$ .

We know that the optical  $\text{TiO}_2/\text{CdS}/\text{CdSe}/\text{ZnS}$  photoanode becomes important for prepared photovoltaic. Fig. 3b shows the UV-Vis absorption spectra of photoanodes measured after each cycle of SILAR. As expected, the absorbance increased with the increased cycles of CdS and CdSe. However, only absorption spectra with SILAR cycles of the  $\text{TiO}_2/\text{CdS}(3)/\text{CdSe}(3)/\text{ZnS}(2)$  photoanode shows the best deposition. At under 550 nm wavelength region, the increase of absorption is due to more CdS was loaded on  $\text{TiO}_2/\text{CdS}/\text{CdSe}/\text{ZnS}$  film. From 550 nm to 629 nm, the deposition of higher amounts of CdSe on  $\text{TiO}_2/\text{CdS}/\text{CdSe}/\text{ZnS}$  electrode results in the shift of the absorption peak toward red region. The sizes of QDs are consistent with the sizes measured from the TEM images.

A higher absorption is thus obtained because the absorption spectrum of ZnS complements those of the CdSe and CdS QDs. Furthermore, ZnS acts as a passivation layer to protect the CdS and CdSe QDs from photocorrosion [11]. In order to understand optical properties of the photoanodes, we measured the PL of the  $\text{TiO}_2/\text{CdS}/\text{CdSe}/\text{ZnS}$  photoanodes. Fig 3(c) shows that the PL of the different photoanodes decreased when the ZnS layer grown on top of the CdSe improves the optical properties of the photoanodes by the passivating CdS/CdSe surface defects.

A cascade type of energy band structure is constructed for the co-sensitized photoanodes. The best electron transport path is from the CB of ZnS and CdSe to that of CdS, and finally, to  $\text{TiO}_2$  film (inset in Fig 4b). Thus, the PL of  $\text{TiO}_2/\text{CdS}/\text{CdSe}/\text{ZnS}$  was quenched (displayed in Figure 3(c)). This reveals that the  $\text{TiO}_2$  film serves as effective quenchers of excited CdS, CdSe and ZnS QDs. The thickness photoanode film quenches more efficiently than thin photoanode film.

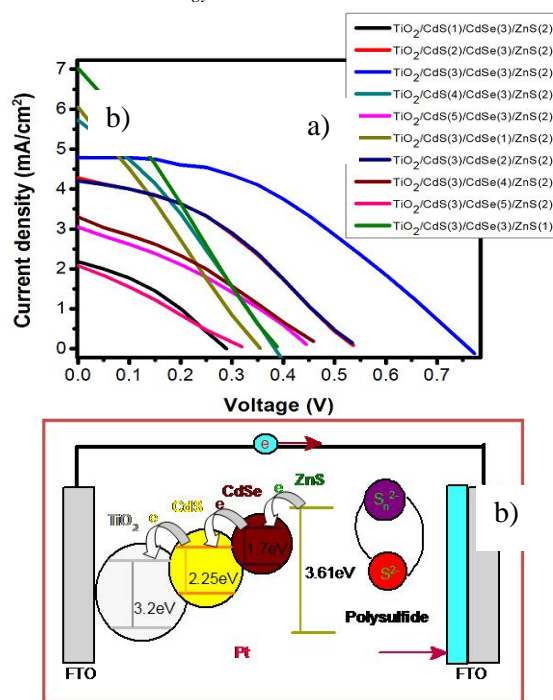


**Fig 4.** (a) The J-V curves of the QDSSCs with different photoanodes under one sun illuminates and (b) diagram shows the values efficiency of solar cells.

The  $\text{TiO}_2/\text{CdS}/\text{CdSe}/\text{ZnS}$  co-sensitized solar cells demonstrated a better performance (1.52%) than the  $\text{TiO}_2/\text{CdS}$  (0.22%) and  $\text{TiO}_2/\text{CdSe}$  QDSSC (0.575%) (shows in Fig 4a) [12]. This suggests that the charge injection from the CdSe conduction level to the  $\text{TiO}_2$  conduction level may not be effective, due to the quasi Fermi levels of CdSe being lower than that of  $\text{TiO}_2$  [13]. However, the quasi Fermi level of CdS quantum dots is higher than that of the  $\text{TiO}_2$  layer [14] and it is expected to improve the charge injection from CdSe to  $\text{TiO}_2$ . Moreover, a ZnS coating forms a potential barrier between the CB from QDs and the electrolyte, which blocks the electrons in the CB from QDs to the electrolyte and reduced the defect states in QDs [13]. So the electron density in the conduction band of QDs increased and the enhanced  $J_{SC}$  is obtained. The Result of a high performance is obtained. In addition, with the increased electron density in the conduction band of QDs, the quasi Fermi level becomes increasing and consequently,  $V_{OC} = (E_{Fn} - E_{F0})/(-q)$  increased. With combination CdS, CdSe, ZnS, the CdS Fermi energy level position is higher than of  $\text{TiO}_2$ , beneficial effects are conferred to the coupled QDSSCs system. It is evident that the parameters of the coupled QDSSCs were influenced by CdS/CdSe/ZnS co-sensitization cycles [13].

To explain this, The CdS, CdSe and ZnS QDs lead to the quasi Fermi level alignment and consequently, results in a cascade energy level structure in the order of  $CB_{\text{TiO}_2} < CB_{\text{CdS}} < CB_{\text{CdSe}} < CB_{\text{ZnS}}$ . That is, the introduction of a CdS layer between  $\text{TiO}_2$  and CdSe elevates the conduction band edge of CdSe, giving a higher driving force for the injection of excited electrons out of the CdSe layer [14]. Further, the photocurrent density might be enhanced with QDs loading by means of increasing coating cycles [15].

**Table 1.** Resistance ( $R_D$ ,  $R_d$ ,  $R_S$ ,  $R_{SH}$ ) of the QDSSCs depending on the cycles of the CdS films were calculated from Eqs (1-4)

Sample	$R_D$ ( $\Omega$ )	$R_d$ ( $\Omega$ )	$R_S$ ( $\Omega$ )	$R_{SH}$ ( $\Omega$ )	Efficiency $\eta$ (%)
TiO <sub>2</sub> /CdS(1)/CdSe(3)/ZnS(2)	58.6	23.1	35.5	5472.1	0.22
TiO <sub>2</sub> /CdS(2)/CdSe(3)/ZnS(2)	132.9	123	32.9	2174.5	0.86
TiO <sub>2</sub> /CdS(3)/CdSe(3)/ZnS(2)	58.7	41.7	17	6040.9	1.52
TiO <sub>2</sub> /CdS(4)/CdSe(3)/ZnS(2)	151.7	35.7	116	3105.5	0.68
TiO <sub>2</sub> /CdS(5)/CdSe(3)/ZnS(2)	157.3	70.2	87.1	2932	0.45

**Table 2.** Resistance ( $R_D$ ,  $R_d$ ,  $R_S$ ,  $R_{SH}$ ) of the QDSSCs depending on the cycles of the CdSe films were calculated from Eqs (1-4)

Sample	$R_D$ ( $\Omega$ )	$R_d$ ( $\Omega$ )	$R_S$ ( $\Omega$ )	$R_{SH}$ ( $\Omega$ )	Efficiency $\eta$ (%)
TiO <sub>2</sub> /CdS(3)/CdSe(1)/ZnS(2)	127.7	36.7	91	4197	0.55
TiO <sub>2</sub> /CdS(3)/CdSe(2)/ZnS(2)	55.5	27.3	28.2	6890.6	0.88
TiO <sub>2</sub> /CdS(3)/CdSe(3)/ZnS(2)	58.7	41.7	17	6040.9	1.52
TiO <sub>2</sub> /CdS(3)/CdSe(4)/ZnS(2)	172.8	33.7	139.1	4666.5	0.50
TiO <sub>2</sub> /CdS(3)/CdSe(5)/ZnS(2)	417.4	193	224.4	726.5	0.18

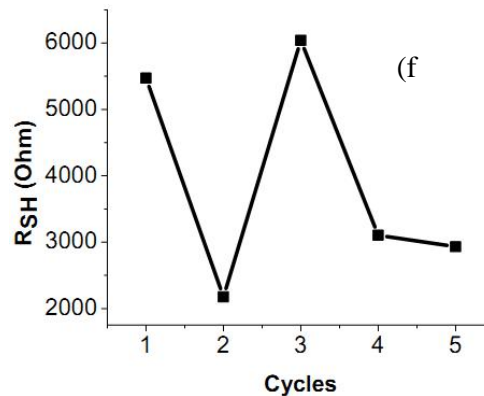
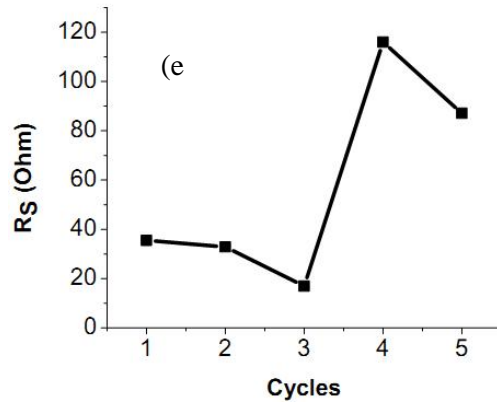
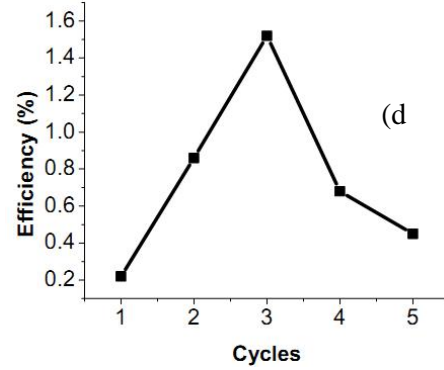
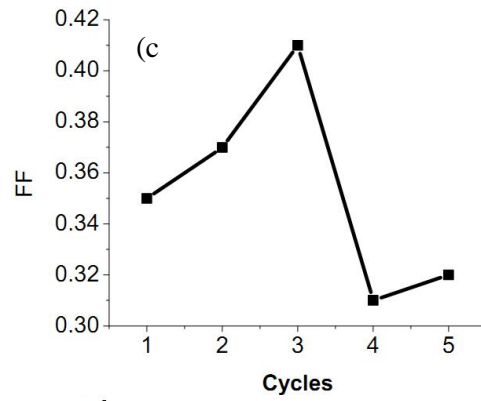
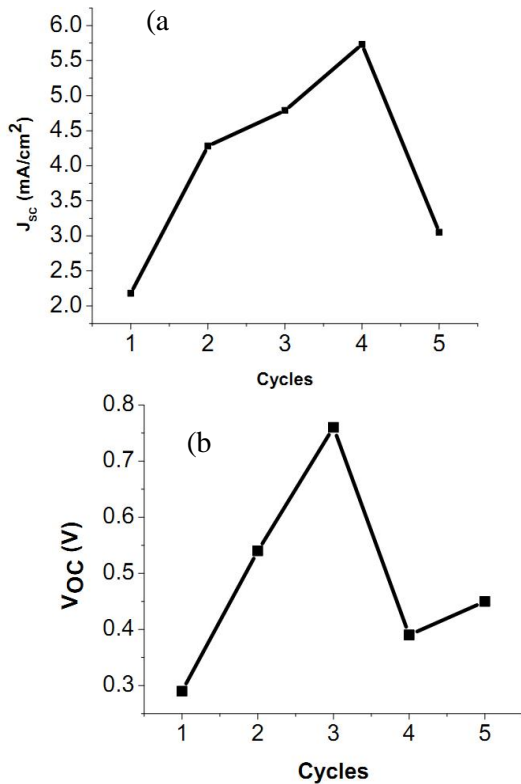


**Fig 5.** Diagrams describe the variation of the parameters characterizing as  $V_{oc}$ ,  $J_{sc}$ , FF,  $\eta$ ,  $R_S$ ,  $R_{SH}$  depending on the cycles of the CdS films.



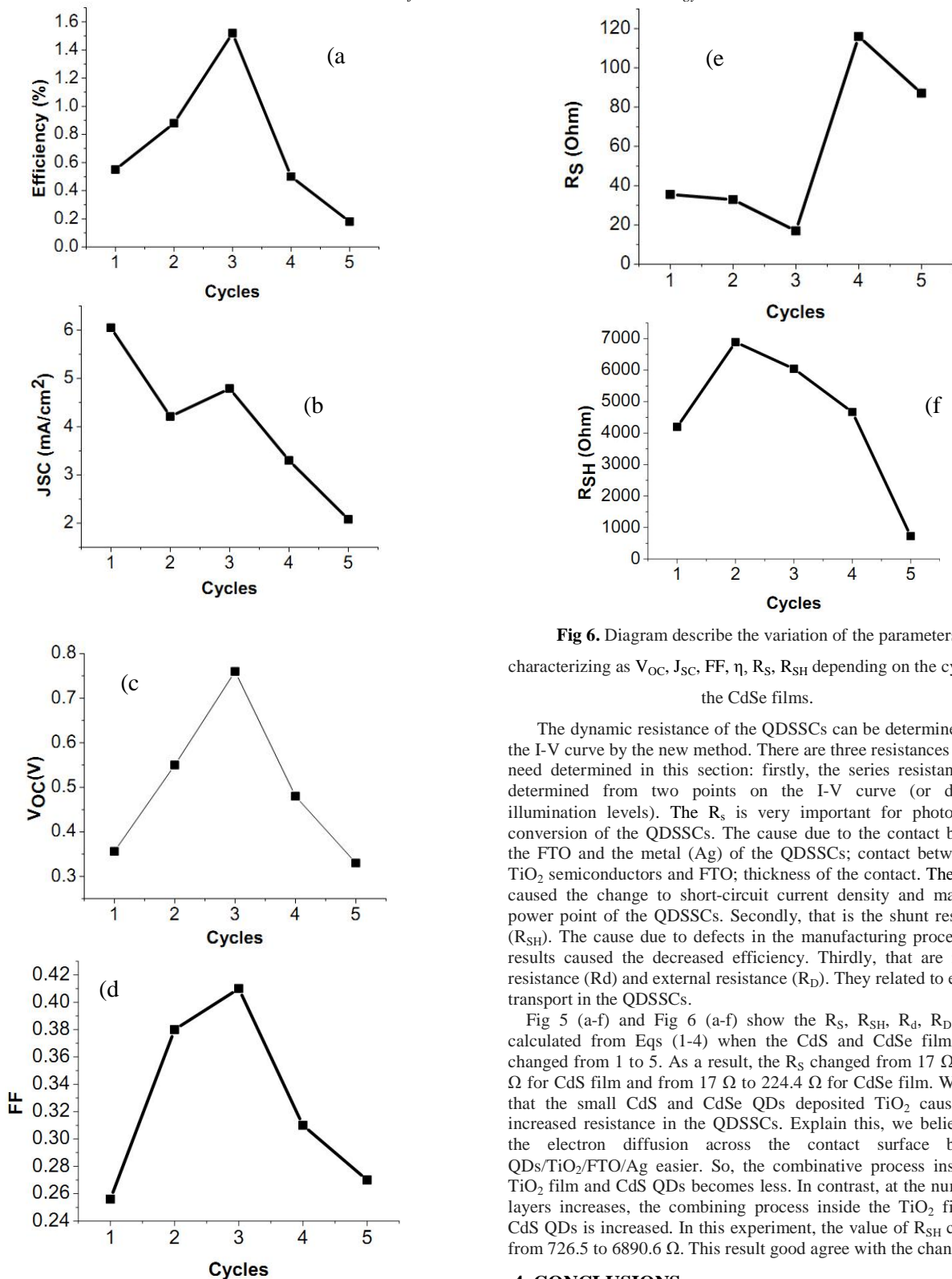


**Fig 6.** Diagram describe the variation of the parameters characterizing as  $V_{OC}$ ,  $J_{SC}$ , FF,  $\eta$ ,  $R_S$ ,  $R_{SH}$  depending on the cycles of the CdSe films.

The dynamic resistance of the QDSSCs can be determined from the I-V curve by the new method. There are three resistances that we need determined in this section: firstly, the series resistance ( $R_s$ ) determined from two points on the I-V curve (or different illumination levels). The  $R_s$  is very important for photoelectric conversion of the QDSSCs. The cause due to the contact between the FTO and the metal (Ag) of the QDSSCs; contact between the TiO<sub>2</sub> semiconductors and FTO; thickness of the contact. The results caused the change to short-circuit current density and maximum power point of the QDSSCs. Secondly, that is the shunt resistance ( $R_{SH}$ ). The cause due to defects in the manufacturing process. The results caused the decreased efficiency. Thirdly, that are internal resistance ( $R_d$ ) and external resistance ( $R_D$ ). They related to electron transport in the QDSSCs.

Fig 5 (a-f) and Fig 6 (a-f) show the  $R_s$ ,  $R_{SH}$ ,  $R_d$ ,  $R_D$  values calculated from Eqs (1-4) when the CdS and CdSe film cycles changed from 1 to 5. As a result, the  $R_s$  changed from 17  $\Omega$  to 116  $\Omega$  for CdS film and from 17  $\Omega$  to 224.4  $\Omega$  for CdSe film. We think that the small CdS and CdSe QDs deposited TiO<sub>2</sub> causing the increased resistance in the QDSSCs. Explain this, we believe that the electron diffusion across the contact surface between QDs/TiO<sub>2</sub>/FTO/Ag easier. So, the combinative process inside the TiO<sub>2</sub> film and CdS QDs becomes less. In contrast, at the number of layers increases, the combining process inside the TiO<sub>2</sub> film and CdS QDs is increased. In this experiment, the value of  $R_{SH}$  changed from 726.5 to 6890.6  $\Omega$ . This result good agree with the changed  $R_s$ .

#### 4. CONCLUSIONS

In conclusion, we successfully fabricated a TiO<sub>2</sub> photoanode which is sequentially modified with CdS, CdSe and ZnS QDs. A series of the CdS/CdSe/ZnS co-sensitized TiO<sub>2</sub> photoanodes for QDs sensitized solar cells were prepared by SILAR processes. We have evaluated the number of CdS, CdSe and ZnS SILAR cycles effect on the optical and electronic properties of the QDSSCs. The

increasing SILAR cycles of both CdS and CdSe lead to an increasing in the light absorption but they show different impacts on the performance of QDSSC. This improvement is mainly attributed to the overlap of the absorption spectra of the different materials and the formation of an ideal stepwise band structure which promotes the transport of excited electrons and holes across the composite electrodes. When the changed CdS and CdSe film cycles from 1 to 5, the  $R_s$  changed from 17  $\Omega$  to 116  $\Omega$  for CdS film and from 17  $\Omega$  to 224.4  $\Omega$  for CdSe film.

## ACKNOWLEDGMENTS

This work was supported by Vietnam National University by the name of the project: B 2012-18-5TD, the University of Science of Ho Chi Minh City and Dong Thap University.

## REFERENCES

- [1] Shen Q, Arae D, Toyoda T, *Photosensitization of nanostructured TiO<sub>2</sub> with CdSe quantum dots: effects of microstructure and electron transport in TiO<sub>2</sub> substrates*. Journal of Photochemistry and Photobiology A: Chemistry **164**,75–80 (2004).
- [2] Robel, István, Kuno. M, and Kamat. P. V, *Size-dependent electron injection from excited CdSe quantum dots into TiO<sub>2</sub> nanoparticles*. Journal of the American Chemical Society **129** (14). 4136-4137 (2007).
- [3] Peng, Adam. Z and Peng. P, *Formation of high-quality CdTe, CdSe, and CdS nanocrystals using CdO as precursor*. Journal of the American Chemical Society **123**(1). 183-184 (2001).
- [4] Vogel, Ralf, Pohl. K and Weller. H, *Sensitization of highly porous, polycrystalline TiO<sub>2</sub> electrodes by quantum sized CdS*. Chemical Physics Letters **174** (3), 241-246 (1990).
- [5] Lee H-J, Kim D-Y, Yoo J-S, Bang J, Kim S, Park S-M, *Anchoring cadmium chalcogenide quantum dots (QD) onto stable oxide semiconductor for QD sensitized solar cells*. Bulletin of the Korean Chemical Society **28**, 953–8 (2007).
- [6] Lee H-J, Yum J-H, Leventis HC, Zakeeruddin SM, Haque SA, Chen P, Seok SI, Gratzel M, Nazeeruddin M-K, *CdSe quantum dot-sensitized solar cells exceeding efficiency 1% at full sun intensity*. Journal of Physical Chemistry C **112**, 11600–8 (2008).
- [7] Lee WJ, Kang SH, Min S-K, Sung Y-E, Han S-H, *Co-sensitization of vertically aligned TiO<sub>2</sub> nanotubes with two different sizes of CdSe quantum dots for broad spectrum*. Electrochemistry Communications **10**,1579–82 (2008).
- [8] Kim. J. Y, Lee. K, Coates. N. E, Moses. D, Nguyen. T. Q, Dante. M and Heeger. A. J, *Efficient tandem polymer solar cells fabricated by all-solution processing*. Science **317** (5835), 222-225 (2007).
- [9] Cheng. S, Fu. W, Yang. H, Zhang. L, Ma. J, Zhao. H, Sun. M, Yang. L, *Photoelectrochemical performance of multiple semiconductors (CdS/CdSe/ZnS) cosensitized TiO<sub>2</sub> photoelectrodes*. Journal of Physical Chemistry C **116**, 2615–21 (2012).
- [10] J.T hongpron, K. Kirtikara, and C. Jivacate, *A method for the determination of dynamic resistance of photovoltaic modules under illumination*. in Proceedings of the Technical Digest of the 14th International Photovoltaic Science and Engineering Conference (PVSEC1404), Bangkok, Thailand, January. 2004.
- [11] Tachan. Z, Shalom. M, Hod. I, Ruhle. S, Tirosh. S and Zaban. A, J. Phys. Chem. C **115**, 6162 (2011).
- [12] Chang. C. H, Lee. Y. L. Appl. Phys. Lett **91**, 053503 (2007).
- [13] Balisa. N, Dracopoulosb. V, Bourikasc. K, Lianos. P, *Quantum dot sensitized solar cells based on an optimized combination of ZnS, CdS and CdSe with CoS and CuS counter electrodes*. Electrochimica Acta **91**, 246–252 (2013).
- [14] Kim. J. Y, Choi. S. B, Noh. J. H, Yoon. S. H, Lee. S.W, Noh. T.H, Frank. A.J, Hong. K.S. Langmuir **25**, 5348 (2009).
- [15] CHRIS. G. V AND NEUGEBAUER. J. NATURE **423**, 626 (2003).